A developmental and energetic basis linking larval oyster shell formation to acidification sensitivity

George G. Waldbusser,[1] Elizabeth L. Brunner,[1] Brian A. Haley,[1] Burke Hales,[1] Christopher J. Langdon,[2] and Frederick G. Prahl[1]

Received 31 January 2013; revised 4 April 2013; accepted 4 April 2013; published 29 May 2013.

[1] Acidified waters are impacting commercial oyster production in the U.S. Pacific Northwest, and favorable carbonate chemistry conditions are predicted to become less frequent. Within 48 h of fertilization, unshelled Pacific oyster (*Crassostrea gigas*) larvae precipitate roughly 90% of their body weight as calcium carbonate. We measured stable carbon isotopes in larval shell and tissue and in algal food and seawater dissolved inorganic carbon in a longitudinal study of larval development and growth. Using these data and measured biochemical composition of larvae, we show that sensitivity of initial shell formation to ocean acidification results from diminished ability to isolate calcifying fluid from surrounding seawater, a limited energy budget and a strong kinetic demand for calcium carbonate precipitation. Our results highlight an important link between organism physiology and mineral kinetics in larval bivalves and suggest the consideration of mineral kinetics may improve understanding winners and losers in a high CO_2 world.
Citation: Waldbusser, G. G., E. L. Brunner, B. A. Haley, B. Hales, C. J. Langdon, and F. G. Prahl (2013), A developmental and energetic basis linking larval oyster shell formation to acidification sensitivity, *Geophys. Res. Lett.*, *40*, 2171–2176, doi:10.1002/grl.50449.

1. Introduction

[2] Several years of oyster seed production failures in the U.S. Pacific Northwest have been linked to wind-driven upwelled waters with elevated P_{CO2} [*Barton et al.*, 2012]. Recent measurements and future projections of carbonate chemistry in the California Current Ecosystem highlight the rapid acidification of coastal waters [*Feely et al.*, 2008; *Gruber et al.*, 2012; *Hauri et al.*, 2012] that are strongly coupled to U.S. Pacific Northwest estuaries [*Hickey and Banas*, 2003; *Barton et al.*, 2012]. In coastal environments, carbonate chemistry may vary widely both spatially and temporally [*Hinga*, 2002; *Hofmann et al.*, 2011; *Waldbusser et al.*, 2011] and can result in transient conditions (in excess of global averages) that are unfavorable for sensitive species [*Gruber et al.*, 2012; *Hauri et al.*, 2012]. Many laboratory-based studies have documented the sensitivity of larval bivalves to deleterious carbonate chemistry [*Kurihara et al.*, 2007; *Talmage and Gobler*, 2010; *Miller et al.*, 2009], and more thermodynamically soluble mineral phases in larval shell is often cited for this sensitivity [e.g., *Weiss et al.*, 2002]. However, sensitivities vary strongly as a function of life-history stage and food availability [*Green et al.*, 2009; *Waldbusser et al.*, 2010; *Melzner et al.*, 2011], or on previous exposure of reproductive adults and larvae to acidified waters [*Barton et al.*, 2012; *Hettinger et al.*, 2012; *Parker et al.*, 2012]. A model of organism sensitivity to ocean acidification based on $CaCO_3$ polymorph solubility alone cannot adequately explain these results. Thus, an integrative examination of larval development, mineral dynamics, and early life-history is required.

[3] In adult bivalves, the calcifying fluid, where calcium carbonate is precipitated from, may chemically resemble ambient seawater [*Thomsen et al.*, 2010] or deviate significantly [*Crenshaw*, 1972]. Bivalves are osmoconformers [*Shumway*, 1977] but do have limited control of their calcifying fluid [*Nair and Robinson*, 1998]. Because mineral precipitation consumes alkalinity and generates protons, the continued formation of calcium carbonate requires the removal of protons from the calcifying fluid. Active modification of the calcifying fluid is also evidenced in the significant contribution of metabolic carbon to precipitated calcium carbonate in some marine bivalves [*Gillikin et al.*, 2007]. In *Crassostrea* spp., the unshelled swimming trochophore develops within 6–10 h of fertilization. An outer organic shell layer called the periostracum begins to form immediately following the trochophore stage and mineral calcification is initiated well in advance of its completion [*Kniprath*, 1981]. A fully formed and calcified larval shell (the prodissoconch I or D-hinge) is completed within 24–48 h [*His and Maurer*, 1988]. Larval shell formed after the D-hinge stage is distinct and called prodissoconch II shell (and also aragonite).

[4] In supersaturated seawater, calcium carbonate precipitation is thermodynamically favored and forms at a rate relative to the saturation state, modeled as

$$r = k(\Omega - 1)^n \quad (1)$$

[5] where r is the mineral precipitation rate, k is the rate constant, Ω is the saturation state with respect to the given mineral, and n is the reaction order [reviewed in *Morse et al.*, (2007)]. We can assume equation (1) provides the fundamental kinetic constraint on biocalcification. Most marine bivalve shell is however mineralized at rates that are much faster than abiotic precipitation in super saturated seawater [*Zuddas and Mucci*, 1998]. Calcifying organisms may overcome this kinetic constraint by the use of organic

[1]College of Earth, Ocean, and Atmospheric Sciences, Oregon State University, Corvallis, Oregon, USA.
[2]Department of Fisheries and Wildlife, Oregon State University, Newport, Oregon, USA.

Corresponding author: George G. Waldbusser, College of Earth, Ocean, and Atmospheric Sciences, Oregon State University, 104 Ocean Admin, Corvallis, OR 97331, USA. (waldbuss@coas.oregonstate.edu)

0094-8276/13/10.1002/grl.50449

macromolecules [*Elhadj et al*. 2006] and by membrane/cellular transport pumps [*Cohen and McConnaughey*, 2003]. These strategies must also be physiologically and energetically constrained by the degree to which organisms can effectively increase k or Ω.

[6] We therefore propose two hypotheses to explain why oyster larvae appear particularly sensitive to ambient carbonate chemistry during the development of the initial prodissoconch I (D-hinge) shell: (1) the calcifying fluids and surfaces are more exposed to ambient carbonate chemistry conditions until the D-hinge shell is completed and (2) the kinetic demand (or rate) of shell accretion far exceeds possible abiotic precipitation rates even under thermodynamically favorable conditions, thus, mineral precipitation requires significant energy input at a life history stage when energy is limited.

2. Methods

[7] We measured the isotopic composition of carbon in larval shell, larval tissue, food, and holding tank water during growth and development of a commercial larval *Crassostrea gigas* cohort in May 2011. We coupled these measurements to bulk measures of larval biochemical composition to estimate energetic status and demands for the initial shell development.

2.1. Setting and Experimental Design

[8] *Crassostrea gigas* larvae were raised according to commercial spawning protocols at Whiskey Creek Shellfish Hatchery in Netarts Bay, Oregon, as previously described in detail in [*Barton et al*., 2012]. Briefly, successfully fertilized Willapa Bay oyster larvae from several conditioned broodstock oysters were added to a 22 m^3 tank an hour after fertilization at an estimated density of approximately 5×10^7 ind. m^{-3}. Water was changed in culture tanks every 2–3 days during cohort development. The pH of fertilization water was 8.15 (measured with a YSI 30 on the NBS scale), and developing embryos were reared under a P_{CO2} of 396 µatm and aragonite saturation state of 2.38. Samples for P_{CO2} and TCO_2 of culture tanks were collected at each tank filling and analyzed following *Bandstra et al*. [2006] with an uncertainty of less than 5% and 0.2% for P_{CO2} and TCO2, respectively. The rest of the carbonate system was calculated using standard dissociation constants as previously described [*Barton et al*., 2012]. Conditions in culture tanks at filling had an average P_{CO2} (±1 S.D.) of 364 (±40) µatm aragonite saturation state with 2.58 (±0.33) at the culture temperature of 25 °C, and a salinity of 26.5 (±2.29). Larvae were fed a diet of *Isocrysis galbani* cultured in a continuous culture system during the first week following fertilization, and this was switched to a mixed algae diet consisting primarily of *Chaetocerous gracilis*, *Thalassiorsira* spp., and *Isochrysis galbana* cultured in batches. Estimated cell densities were $5–7 \times 10^{10}$ cells m^{-3}.

[9] During each tank change, all larvae were captured on an appropriately sized sieve, and a primary sample of the entire cohort was randomly collected with a clean stainless steel spatula. The mass of each primary sample varied from ~0.5 to 1.0 g representing an estimated 2.8×10^6 to 5.6×10^6 two day old larvae or 2.3×10^5 to 4.6×10^5 19 day old larvae. All 400 million larvae in the cohort were reared collectively in one tank, so replicate primary samples would have been pseudo-replicates of larvae from the same tank.

[10] The larval samples were quickly rinsed with deionized water, immediately frozen, and freeze dried within 2 weeks with a Labconco FreeZone 6 Freeze Drier. Subsamples from each primary sample were then used for subsequent analyses. Approximately 100s to 10s of larvae for stable isotope analyses of shell carbonates from day 2 and 19 samples were needed, and lipid extractions required roughly 10^4 to 10^5 larvae for day 2 and 19, respectively. Analyses of stable isotopes and elemental analyses of tissue required approximately 10^3 to 10^4 larvae. Variable volumes (200–800 ml) of algal cultures were vacuum filtered onto pre-combusted onto glass fiber filters (GF/F 47 mm, Whatman) to achieve a similar analytical mass for all analyses.

2.2. $\delta^{13}C$ Measurements

[11] All stable carbon isotope samples were analyzed in Oregon State University's CEOAS Stable Isotope Laboratory and details for standard analyses may be found here (http://stable-isotope.coas.oregonstate.edu/). All runs were calibrated and checked with NIST certified (NBS 19, NBS 20 UQ6) and in-house calibrated standards, with precision and accuracy noted below.

[12] Water samples were analyzed by continuous mass flow spectrometry on a GasBench-Delta V system. The run had a precision of 0.02‰ and accuracy better than 0.06‰. Larval shell carbonate $\delta^{13}C$ was measured by reacting the freeze-dried larvae with a viscous ~105% H_3PO_4 solution in a Finnigan MAT Kiel III at 70 °C for 5 min after which the isotopic composition of the evolved and purified CO_2 was measured on a dual inlet mass spectrometer (MAT 252 IRMS). Each run had a precision and accuracy of 0.02‰ and 0.01 ‰, respectively. Repeatability of larval shell samples was within 0.02‰. To obtain measures of tissue $\delta^{13}C$ composition of tissues, freeze-dried larvae were acid fumed with concentrated HCl to eliminate the shell carbonate signal. The remaining sample material was then analyzed by flash combustion (>1000 °C) using a Carlo Erba NA 1500 elemental analyzer interfaced by continuous-flow mass spectrometer (Delta-Plus XL). Repeatability of organic larval samples was 0.21‰. Algae samples, collected as noted above, were analyzed in the same way as larval tissue however without the acid fuming. Measurements of organic $\delta^{13}C$ composition were made with a precision and accuracy of 0.17‰ and 0.12‰, respectively.

2.3. Larval Biochemical and Size Analyses

[13] Fractions of organic tissue and shell (% of dry weight) were determined by first measuring %C on bulk freeze-dried larval samples and then decalcified samples (via HCl fuming) on a Carlo Erba NA1500 elemental analyzer. The difference between whole and decalcified larvae and the molar proportion of C in calcium carbonate were used to estimate the percent calcium carbonate by weight, with the remainder being organic matter. These values for percent organic matter were correlated to ($r^2 = 0.89$) loss on ignition (LOI) measurements, with LOI consistently over estimating percent organic matter. Total lipid percent was measured by extracting freeze-dried larvae with a methylene chloride: methanol solution (3:1) using a Dionex ASE 200 Accelerated Solvent Extractor and weighing an aliquot of the isolated total extractable lipid (TEL) fraction dissolved in CS_2 gravimetrically. Larval size was evaluated on 100–150 larvae per sample, taken as a separate subsample during tank water changes and evaluated on

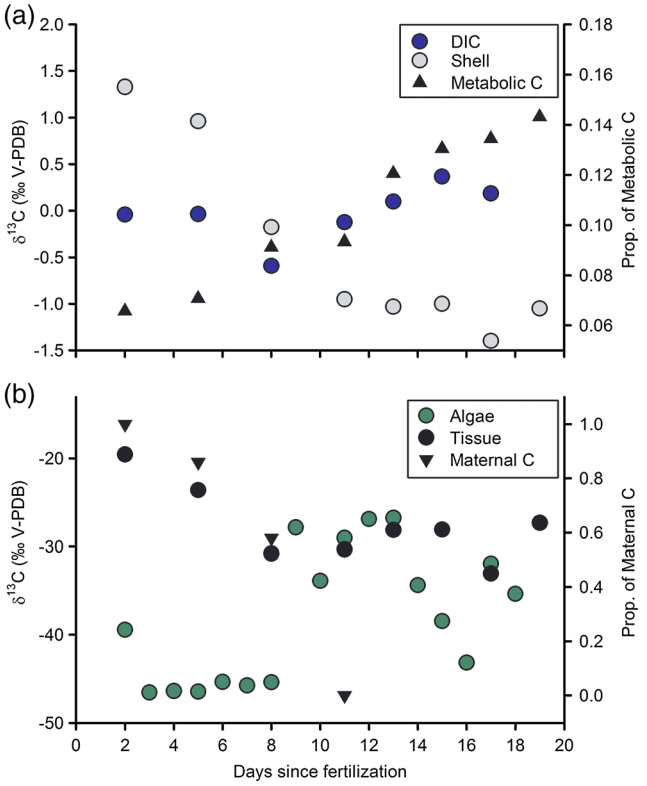

Figure 1. Stable carbon isotope ($\delta^{13}C$) values in (a) larval shell and ambient DIC and (b) tissue and algal food. The right axis and triangles are estimated metabolic C contribution to shell (Figure 1a), and the proportion of maternally derived C in tissue (Figure 1b). The large shift in $\delta^{13}C_{algae}$ at day 9 corresponds to a change from an Isochrysis strain (C-ISO) food reared in a continuous-culture closed bag system to a mixed diet in batch culture.

digital micrographs using standard image analysis techniques (ImageJ 1.44p). A standard mass at length model for *C. gigas* larvae [*Bochenek et al.*, 2001] was used to calculate a total individual mass. Measured proportional composition data were then applied to the mass at length estimate to compute per larva weights of shell, bulk organic, and lipid content.

3. Results

[14] The $\delta^{13}C_{shell}$ of *C. gigas* larvae shifted from +1.5 ‰ 48 hours after fertilization (immediately after the prodissoconch I stage) to −1 ‰ by 11 days (prodissoconch II), indicating a shift away from ^{13}C-enriched seawater dissolved inorganic carbon (DIC) to ^{13}C-depleted metabolically respired carbon in the larval shell (Figure 1). Metabolic carbon in shell carbonate doubled from ~7% on day 2 to ~14% on day 14 post-fertilization (Figure 1), calculated following [*McConnaughey et al.*, 1997] as:

$$R\left(\delta^{13}C_{Resp}\right) + (1-R)\left(\delta^{13}C_{DIC}\right) = \delta^{13}C_{Shell} - \Delta \qquad (1)$$

[15] where R is the proportion of metabolic contribution to shell, $\delta^{13}C_{Resp}$ is the isotope value of respired carbon approximated from larval organic tissue; $\delta^{13}C_{DIC}$ is the isotope value of the ambient DIC; $\delta^{13}C_{shell}$ is the isotope value of the shell, and Δ is the abiotic fractionation between aragonite and bicarbonate [*Romanek et al.*, 1992].

[16] At fertilization, oyster embryos are entirely organic material and by 2 days post-fertilization, the shelled larvae have precipitated ~160 ng $CaCO_3$ larva^{-1}, constituting >90% of total larval mass. The mass-normalized shell precipitation rate in this first 2 days is 0.45 d^{-1}, and decreases by an order of magnitude by day 5 to 0.04 d^{-1} (Figure 2a). Formation of the initial shell occurs with little to no new growth in tissue; organic mass remained constant from day 2 to 5 at 16 ng larva^{-1}, and lipids do not begin to accumulate until 11 days post fertilization, following a minimum of 2.6 ng larva^{-1} (Figure 2b).

[17] Our measurements of $\delta^{13}C_{tissue}$ show the slow transition from endogenous energy sources derived from egg reserves to exogenous food sources for developing bivalve larvae by the large deviation of tissue from algal food sources during the first week following fertilization (Figure 1b). The

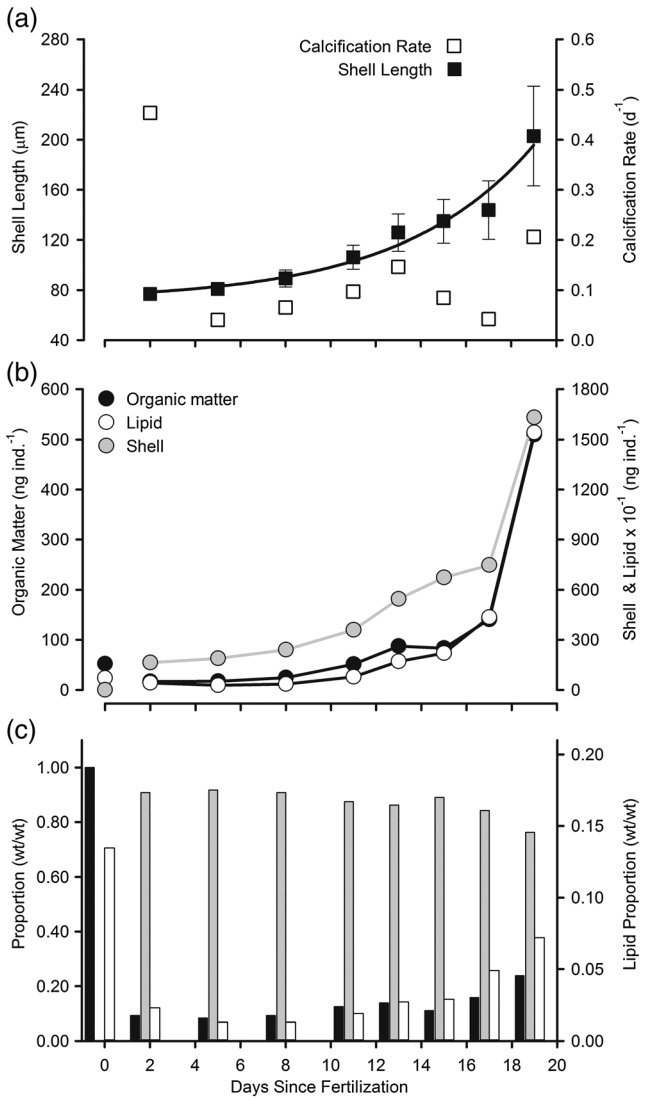

Figure 2. (a) Growth and (b) composition of oyster larvae. Calcification rate is mass normalized. Error bars are standard deviations. Bulk organic matter, shell, and lipid content in ng larva^{-1} are shown in Figure 2b. Day zero (egg) values are from published sources [e.g., *Gallager and Mann*, 1986] to illustrate a typical egg composition. (c) Bar colors correspond to those in Figure 2b.

deviation between food and tissue between days 14–16 is likely related to changes in feeding associated with a change in algal diet, which is concurrent with a decrease in growth and calcification (Figure 2a) and a slight shift in $\delta^{13}C_{shell}$ as would be expected if calcification rate slowed [*Gillikin et al*., 2007]. $\delta^{13}C_{egg}$ of *C. gigas* eggs from another cohort produced in the hatchery was −20‰. Assuming a simple two-member mixing model of food sources; egg and algae, and no trophic enrichment [*McCutchan et al*., 2003], the contribution of egg derived carbon to larval tissue growth is 100% on day 2 decreasing to 86%, 58%, and 0% on days 5, 8, and 11, respectively. These results highlight that initial shell production in oyster larvae is supported by the limited energy reserves of eggs.

4. Discussion and Conclusions

[18] Greater incorporation of DIC from ambient seawater during D-hinge shell formation (Figure 1a) and the developmental biology of bivalve larvae [*Kniprath*, 1981] suggest two non-exclusive posits: developing D-hinge larvae cannot isolate the calcifying space as easily as later stage larvae, and under high rates of shell precipitation, more DIC is needed. Both of these indicate that during initial shell formation, the calcification surfaces will be more exposed and dependent on seawater carbonate speciation. Adult bivalves are known to incorporate a small but significant fraction of metabolic carbon into their shells and this fraction generally increases with age, slowed growth/calcification, or increased food supply [*Lorrain et al*., 2004; *McConnaughey and Gillikin*, 2008; *Lartaud et al*., 2010]. Such ontogenic changes have not been previously documented in developing bivalve larvae, but it should be noted that our observational study is based on one cohort (from multiple parents). Ongoing studies of other larval cohorts show only minor variations from the $\delta^{13}C$ patterns reported here and these appear diagnostic of larval fitness, confirming our findings. These results will be reported in a future manuscript.

[19] During the formation of the initial D-hinge shell, larval oysters must precipitate calcium carbonate at a rate greater than abiotic precipitation [*Zuddas and Mucci*, 1998] and an order of magnitude greater than later larval stages (Figure 2a). If we assume first order ($n = 1$) precipitation kinetics (e.g., $r = k[\Omega - 1]$ as above), at the mass-normalized mineral precipitation rates ($r = 0.45$ and $0.04\ d^{-1}$) for initial and later shell stages, respectively, an exponential increase in the difference between k to maintain each precipitation rate is found as aragonite saturation state (Ω) approaches 1 (saturation). It is important to note that in this formulation, precipitation rates would be better described as per surface area (rather than mass) [*Morse et al*., 2007], however, surface area estimates of calcification surfaces are lacking. Mollusks employ two strategies to overcome the kinetic constraint: (1) use of organic molecules that increase rates of mineral formation [*Elhadj et al*., 2006] and (2) increase of proton pumping [*Ries* 2011] to elevate saturation state at the mineral formation sites. Both of these strategies require energy, and it is unclear to what extent each is employed during and following D-hinge shell formation. The initial shell appears to be formed with less ability to isolate the site of calcification (highlighted by the shift in $\delta^{13}C_{shell}$). Following D-hinge formation, this kinetic constraint is greatly reduced as the rate of shell formation decreases, while feeding and shell-forming organs develop providing means to reduce acidification stress [*Waldbusser et al*., 2010].

[20] The formation of calcium carbonate removes carbonate ions from seawater and results in the formation of protons within the calcifying fluids. The number of protons generated by calcium carbonate formation depends on the carbonate system speciation. With bicarbonate generally constituting 85-90% of seawater DIC, we can assume that the protons pumped to mineral precipitation ratio will be ~1 [*Cohen and Holcomb*, 2009] with an increasing ratio as metabolic CO_2 incorporation into the shell increases. At 2 days post-fertilization, larval shell mass was estimated at 162 ng (Figure 2). Assuming a calcium-ATP linked proton pump [*Cohen and Holcomb*, 2009] (2 mol H^+ = 1 mol ATP), 1 mol $CaCO_3$ = 1 mol H^+, and using an estimated available energy from converting ATP to ADP of 30 KJ mol^{-1}, the estimated cost of precipitating ~160 ng of $CaCO_3$ is ~24 μJ. If the calcifying fluid during D-hinge shell formation is in greater contact with seawater (as evidenced by the shell isotopes), then proton pumping may be a less important strategy to elevate calcification rate and k must be increased further (presumably by the use of macromolecules). The greater energetic cost is in fact protein synthesis for the shell organic matrix [*Palmer*, 1992]; based on an estimate of 1.9% organic material in the two day old larval shell, and a total shell mass of 162 ng $larva^{-1}$, we estimate this cost to be 70 μJ $larva^{-1}$(following *Palmer* [1992]). The individual energetic cost associated with building the 2 day old shell in our measured cohort can be estimated to be almost 100 μJ $larva^{-1}$.

[21] Our $\delta^{13}C_{tissue}$ isotopic data showing sole utilization of maternally derived carbon during the formation of the initial D-hinge shell (Figure 1b) confirms previous findings on the role of endogenous energy sources for early larval bivalves [*Gallager and Mann*, 1986; *Sanchez-Lazo and Martinez-Pita*, 2012]. The depletion of larval energy reserves (primarily lipids) following D-hinge shell formation (Figure 2b and 2c), and the $\delta^{13}C_{tissue}$ trend (Figure 1b) highlights that the energy available for embryogenesis and D-hinge shell growth is limited by the available maternally-derived energy. Previous measurements of total lipid content of *C. gigas* and other *Crassostrea* spp. eggs found a maximum lipid content of 10 ng egg^{-1} [*Gallager and Mann*, 1986; *His and Maurer*, 1988]; with 1 day old *C. gigas* non-structural lipids (triacylglycerides) comprising greater than half (3.8 ng $larva^{-1}$) of the total lipid pool (5.9 ng $larva^{-1}$) [*Moran and Manahan*, 2004]. Assuming a minimum structural (phospholipid) lipid concentration of ~2 ng $larva^{-1}$ at 1–2 days old, the remaining 8 ng of lipids would therefore provide a total of ~316 μJ $larva^{-1}$ (39.5 μJ per ng lipid). Shell formation of two-day old *C. gigas* therefore would require a minimum of 30% of the total available energy in egg reserves (~100 μJ larva from above), assuming lipid rich eggs. *Crassostrea virginica* larval survival and growth drop quickly when egg lipids falls below 6 ng egg^{-1} [*Gallager and Mann*, 1986] (or 158 μJ $larva^{-1}$ in lipid energy).

[22] Environmental stressors, such as acidification, create additional energetic costs and lower the scope for growth, particularly if food is limited [*Melzner et al*., 2011]. For bivalve larvae, there are two critical stages when larvae must rely on endogenous energy: during embryogenesis (and prodissoconch I shell formation) and during metamorphosis from larvae to juvenile stages. Chronic acidification stress lowers lipid levels in bivalve larvae as they approach

metamorphosis and results in greater failure of settling larvae [*Talmage and Gobler*, 2010, 2011], while calcification in newly settled juvenile hard clams is more sensitive to acidification than later stages [*Waldbusser et al*., 2010]. Success of bivalves in future higher CO_2 waters will ultimately depend on the timing of these critical life-history stages relative to the frequency and duration of unfavorable carbonate chemistry conditions; chemical conditions that are variable [*Hofmann et al*., 2011], predicted to become less favorable rapidly in some systems [*Gruber et al*., 2012], and result from multiple drivers in coastal zones [*Kelly et al*., 2011]. The energetics and kinetics of biocalcification presented here also explains the seemingly unusual sensitivity of early larval calcification to ambient-water chemistry, that is thermodynamically favorable for precipitation ($\Omega > 1$) [*Barton et al*., 2012]. We suggest that the predictions of winners and losers in a high CO_2 world may be better informed by calcium carbonate kinetics, bioenergetics, ontogeny, and life-history characteristics than by shell mineralogy alone.

[23] **Acknowledgments.** The authors would like to thank S. Cudd, M. Wiegardt, and A. Brown of the Whiskey Creek Shellfish Hatchery for oyster larvae, time, and a platform for this work. The authors would also like to thank M. Sparrow, J. McKay, and A. Ross for their analytical expertise. A previous version of this manuscript was greatly improved by thoughtful and critical feedback by C. Gobler and one anonymous reviewer. This work was supported by the National Science Foundation OCE CRI-OA 1041267 to GGW, BH, CJL, and BAH.

[24] The Editor thanks Christopher Gobler and an anonymous reviewer for their assistance in evaluating this paper.

References

Bandstra, L., B. Hales, and T. Takahashi (2006), High-frequency measurements of total CO_2: Method development and first oceanographic observations, *Mar. Chem.*, *100*(1–2), 24–38.

Barton, A., B. Hales, G. G. Waldbusser, C. Langdon, and R. A. Feely (2012), The Pacific oyster, *Crassostrea gigas*, shows negative correlation to naturally elevated carbon dioxide levels: Implications for near-term ocean acidification effects, *Limnol. Oceanogr.*, *57*(3), 698–710.

Bochenek, E. A., J. M. Klinck, E. N. Powell, and E. E. Hofmann (2001), A biochemically based model of the growth and development of *Crassostrea gigas* larvae, *J. Shellfish Res.*, *20*(1), 243–265.

Cohen, A., and T. A. McConnaughey (2003), in *Reviews in mineralogy and geochemistry Vol. 54: Biomineralization*, P. M. Dove, J. J. DeYoreo, S. Weiner, Eds., pp. 151–187, Mineralogical Society of America, Washington, DC.

Cohen, A. L., and M. Holcomb (2009), Why corals care about ocean acidification: uncovering the mechanism, *Oceanography*, *22*(4), 118–127.

Crenshaw, M. A. (1972), Inorganic composition of molluscan extrapallial fluid, *Biol. Bull.*, *143*(3), 506–512.

Elhadj, S., J. J. De Yoreo, J. R. Hoyer, and P. M. Dove (2006), Role of molecular charge and hydrophilicity in regulating the kinetics of crystal growth, *Proc. Natl. Acad. Sci. U.S.A.*, *103*(51), 19237–19242.

Feely, R. A., C. L. Sabine, J. M. Hernandez-Ayon, D. Ianson, and B. Hales (2008), Evidence for upwelling of corrosive "acidified" water onto the continental shelf, *Science*, *320*(5882), 1490–1492.

Gallager, S. M., and R. Mann (1986), Growth and survival of larvae of *Mercenaria mercenaria* (L.) and *Crassostrea virginica* (Gmelin) relative to broodstock conditioning and lipid content of eggs, *Aquaculture*, *56*(2), 105–121.

Gillikin, D. P., A. Lorrain, L. Meng, and F. Dehairs (2007), A large metabolic carbon contribution to the delta C-13 record in marine aragonitic bivalve shells, *Geochim. Cosmochim. Acta*, *71*(12), 2936–2946.

Green, M. A., G. G. Waldbusser, S. L. Reilly, K. Emerson, and S. O'Donnell (2009), Death by dissolution: Sediment saturation state as a mortality factor for juvenile bivalves, *Limnol. Oceanogr.*, *54*(4), 1037–1047.

Gruber, N., C. Hauri, Z. Lachkar, D. Loher, T. L. Fralicher, and G.-K. Plattner (2012), Rapid progression of ocean acidification in the California Current System, *Science*, *337*(6091), 220–223.

Hauri, C., N. Gruber, M. Vogt, S. C. Doney, R. A. Feely, Z. Lachkar, A. Leinweber, A. M. P. McDonnell, M. Munnich, and G. K. Plattner (2012), Spatiotemporal variability and long-term trends of ocean acidification in the California Current System, *Biogeosciences Discuss.*, *9*, 10371–10428, doi:10.5194/bgd-9-10371-2012.

Hettinger, A., E. Sanford, T. M. Hill, A. D. Russell, K. N. S. Sato, J. Hoey, M. Forsch, H. Page, and B. Gaylord (2012), Persistent carry-over effects of planktonic exposure to ocean acidification in the Olympia oyster, *Ecology*, *93*, 2758–2768, doi:10.1890/12-0567.1.

Hickey, B. M., and N. S. Banas (2003), Oceanography of the US Pacific Northwest Coastal Ocean and estuaries with application to coastal ecology, *Estuaries*, *26*(4B), 1010–1031.

Hinga, K. R. (2002), Effects of pH on coastal marine phytoplankton, *Mar. Ecol. Prog. Ser.*, *238*, 281–300.

His, E., and D. Maurer (1988), Shell growth and gross biochemical-composition of oyster larvae (*Crassostrea gigas*) in the field, *Aquaculture*, *69*(1–2), 185–194.

Hofmann, G. E., et al. (2011), High-frequency dynamics of ocean pH: A multi-ecosystem comparison, *PLoS One*, *6*(12), e28983.

Kelly, R. P., M. M. Foley, W. S. Fisher, R. A. Feely, B. S. Halpern, G. G. Waldbusser, and M. R. Caldwell (2011), Mitigating local causes of ocean acidification with existing laws, *Science*, *332*(6033), 1036–1037.

Kniprath, E. (1981), Ontogeny of the molluscan shell field—A review, *Zool. Scr.*, *10*(1), 61–79.

Kurihara, H., S. Kato, and A. Ishimatsu (2007), Effects of increased seawater pCO(2) on early development of the oyster *Crassostrea gigas*, *Aquat. Biol.*, *1*(1), 91–98.

Lartaud, F., L. Emmanuel, M. de Rafelis, S. Pouvreau, and M. Renard (2010), Influence of food supply on the delta C-13 signature of mollusc shells: implications for palaeoenvironmental reconstitutions, *Geo-Mar. Lett.*, *30*(1), 23–34.

Lorrain, A., Y. M. Paulet, L. Chauvaud, R. Dunbar, D. Mucciarone, and M. Fontugne (2004), $\delta^{13}C$ variation in scallop shells: Increasing metabolic carbon contribution with body size?, *Geochim. Cosmochim. Acta*, *68*(17), 3509–3519.

McConnaughey, T. A., and D. P. Gillikin (2008), Carbon isotopes in mollusk shell carbonates, *Geo-Mar. Lett.*, *28*(5–6), 287–299.

McConnaughey, T. A., J. Burdett, J. F. Whelan, and C. K. Paull (1997), Carbon isotopes in biological carbonates: Respiration and photosynthesis, *Geochim. Cosmochim. Acta*, *61*(3), 611–622.

McCutchan, J. H., W. M. Lewis, C. Kendall, and C. C. McGrath (2003), Variation in trophic shift for stable isotope ratios of carbon, nitrogen, and sulfur, *Oikos*, *102*(2), 378–390.

Melzner, F., P. Stange, K. Trubenbach, J. Thomsen, I. Casties, U. Panknin, S. N. Gorb, and M. A. Gutowska (2011), Food supply and seawater pCO (2) impact calcification and internal shell dissolution in the blue mussel *Mytilus edulis*, *PLoS One*, *6*(9), e24223.

Miller, A. W., A. C. Reynolds, C. Sorbino, and G. F. Riedel (2009), Shellfish face uncertain future in high CO_2 world: Influence of acidification on oyster larvae calcification and growth in estuaries, *PLoS Biol.*, *4*(5), e5661.

Moran, A. L., and D. T. Manahan (2004), Physiological recovery from prolonged 'starvation' in larvae of the Pacific oyster *Crassostrea gigas*, *J. Exp. Mar. Biol. Ecol.*, *306*(1), 17–36.

Morse, J. W., R. S. Arvidson, and A. Luttge (2007), Calcium carbonate formation and dissolution, *Chem. Rev.*, *107*(2), 342–381.

Nair, P. S., and W. E. Robinson (1998), Calcium speciation and exchange between blood and extrapallial fluid of the quahog *Mercenaria mercenaria* (L.), *Biol. Bull.*, *195*(1), 43–51.

Palmer, A. R. (1992), Calcification in marine mollusks—How costly is it, *Proc. Natl. Acad. Sci. U. S. A.*, *89*(4), 1379–1382.

Parker, L. M., P. M. Ross, W. A. O'Connor, L. Borysko, D. A. Raftos, and H. O. Portner (2012), Adult exposure influences offspring response to ocean acidification in oysters, *Glob. Change Biol.*, *18*(1), 82–92.

Ries, J. B. (2011), A physicochemical framework for interpreting the biological calcification response to CO_2-induced ocean acidification, *Geochim. Cosmochim. Acta*, *75*(14), 4053–4064.

Romanek, C. S., E. L. Grossman, and J. W. Morse (1992), Carbon isotope fractionaction in synthetic aragonite and calcite: effects of temperature and precipitation rate, *Geochim. Cosmochim. Acta*, *56*(1), 419–430.

Sanchez-Lazo, C., and I. Martinez-Pita (2012), Biochemical and energy dynamics during larval development of the mussel *Mytilus galloprovincialis* (Lamarck, 1819), *Aquaculture*, *358–359*, 71–78.

Shumway, S. E. (1977), Effect of salinity fluctuation on the osmotic pressure and Na^{2+}, Ca^{2+}, and Mg^{2+} ion concentrations in the hemolymph of bivalve molluscs, *Mar. Biol.*, *41*(2), 153–177.

Talmage, S. C., and C. J. Gobler (2010), Effects of past, present, and future ocean carbon dioxide concentrations on the growth and survival of larval shellfish, *Proc. Natl. Acad. Sci. U. S. A.*, *107*(40), 17246–17251.

Talmage, S.C., and J. Gobler (2011), Effects of elevated temperature and carbon dioxide on the growth and survival of larvae and juvenilles of three species of northwest Atlantic bivalves. *PLoS One 6*(10), e26941, doi:10.1371/journal.pone.0026941.

Thomsen, J., et al. (2010), Calcifying invertebrates succeed in a naturally CO_2-rich coastal habitat but are threatened by high levels of future acidification, *Biogeosciences*, *7*(11), 3879–3891.

Waldbusser, G. G., H. Bergschneider, and M. A. Green (2010), Size-dependent pH effect on calcification in post-larval hard clam *Mercenaria* spp, *Marine Ecological Progress Series*, *417*, 171–182.

Waldbusser, G. G., E. P. Voigt, H. Bergschneider, M. A. Green, and R. I. E. Newell (2011), Biocalcification in the eastern oyster (*Crassostrea virginica*) in relation to long-term trends in Chesapeake Bay pH, *Estuaries Coasts*, *34*(2), 221–231.

Weiss, I. M., N. Tuross, L. Addadi, and S. Weiner (2002), Mollusc larval shell formation: Amorphous calcium carbonate is a precursor phase for aragonite, *J. Exp. Zool.*, *293*(5), 478–491.

Zuddas, P., and A. Mucci (1998), Kinetics of calcite precipitation from seawater: II. The influence of the ionic strength, *Geochim. Cosmochim. Acta*, *62*(5), 757–766.